Spectral Simulations Incorporating Gradient Coherence Selection

Karl Young, Gerald B. Matson,* Varanavasi Govindaraju, and Andrew A. Maudsley

*Department of Radiology and *Department of Pharmaceutical Chemistry, University of California at San Francisco, and MR Unit (114M), DVA Medical Center, 4150 Clement Street, San Francisco, California 94121*

Computer-aided methods can considerably simplify the use of the product operator formalism for theoretical analysis of NMR phenomena, which otherwise becomes unwieldy for anything but simple spin systems and pulse sequences. In this report, two previously available programming approaches using symbolic algebra (J. Shriver, *Concepts Magn. Reson.* 4, 1–33, 1992) and numerical simulation using object-oriented programming (S. A. Smith, T. O. Levante, B. H. Meier, and R. R. Ernst, *J. Magn. Reson. A* 106, 75–105, 1994) have been extended to include the use of gradient operators for simulation of spatially localized NMR spectroscopy and gradient coherence selection. These methods are demonstrated using an analysis of the response of an AX_3 spin system to the STEAM pulse sequence and verified with experimental measurements on lactate.   © 1999 Academic Press

***Key Words:* NMR; spectral simulation; product operator formalism; Mathematica; GAMMA; STEAM.**

INTRODUCTION

The theory of *J* coupling in NMR is well understood, and the evolution of spin coherences under the action of RF pulses can be conveniently described using the product operator formalism (*1, 2*). However, the algebra involved in the analysis of coupled spins for multiple-pulse sequences applied to compounds with more than three or four coupled spins becomes extremely tedious. For these more complex coupled spin cases, computational methods can greatly facilitate the analysis. For example, we recently demonstrated the use of direct numerical simulation (*3, 4*), using the publicly available GAMMA library (*5*). Other recent examples of direct numerical simulation also exist (*4, 6*). In addition, it has been shown that symbolic algebra packages such as Mathematica can be used to perform the product operator calculations (*7*).

While either of these two different computational approaches may be used to simulate the observed NMR response, they are also complementary. In general, numerical simulations are considerably faster, require less memory, and can be carried out for complex systems that would be difficult to simulate symbolically. On the other hand, direct inspection of the algebraic terms in a representation of the density matrix operator can provide insight into the evolution of individual coherence terms as well as provide their contributions to the resultant

NMR signal. This capability can be useful for designing sequences to select specific coherence transfer pathways (*8*).

There are many situations where an accurate spectral simulation of complex systems is desirable, for example, to provide *a priori* information for parametric spectral analysis (*9*) and to adjust pulse sequence parameters to optimize observation of a particular compound (*10*). Our previous use of the GAMMA library was for generation of the *a priori* spectral information (frequencies, relative amplitudes, and phases) for known tissue metabolites when subjected to a particular localization sequence (*3*). This information was then used for the basis functions in a parametric analysis of *in vivo* ^{1}H spectra obtained from human brain. This simulation approach provides accurate information for each compound for which the *J* coupling and chemical shift values are known. The simulation approach offers considerable flexibility, enabling spectral information to be easily generated for any pulse sequence, parameter set, and field strength (*3*).

The GAMMA library uses a density matrix description of the spin system and provides an object-oriented programming approach for the simulation of NMR experiments. However, the density matrix description of a spin system does not inherently include the ability to account for spatially dependent variables that are necessary to simulate a number of NMR acquisition sequences, including those used for spatial localization. This capability can be incorporated using additional programming, for example, by repeatedly simulating a response for multiple spatial positions, subject to the varying influences of gradients and frequency-selective pulses. However, this approach significantly increases computational requirements. In this report, the capability of the GAMMA library has been extended to enable efficient methods for simulation of gradients. This extended capability was used to simulate the response of an AX_3 system to the STEAM (*11*) spatial localization pulse sequence. Algebraic results have recently been presented for this problem (*12*), which provide a reliable base for comparison of the results presented here. It should be emphasized that the results discussed in this report model the gradients applied between the RF pulses (Fig. 1) and not the localization gradients. It is the effects of the between RF pulse gradients on the resulting spectra that are of interest.

The effects of localization gradients and non-ideal shaped pulses can also be modeled. This can be done by consideration of evolution of the spin system, during application of the shaped pulse, for a number of effective field strengths. By considering separate simulations of the shaped pulse in constant fields, and then summing the results, rather than treating the gradient pulse as an operator, the fact that RF and gradient pulse operators do not commute can be effectively ignored. This, however, is not the subject of this report and will not be discussed further.

There are a number of packages available for performing symbolic product operator calculations (7, 13). In this report the package described by Shriver (7) was modified and extended to include gradient selection operators, and the ability to retain only product operator combinations that could give rise to observable magnetization. This latter step greatly reduced the time and memory requirements for the STEAM simulations of an AX_3 system. Finally, we confirmed the accuracy of the numerical simulations and symbolic computations by comparison with experimental results obtained for lactate (an AX_3 spin system) at 14 T. The longer-term goal of this work is to apply the tools developed to more complicated spin systems, and to other localization experiments. Although there is some duplication of the report of Wilman and Allen (12) with respect to the analysis of the AX_3 spin system, a more detailed experimental verification of the theoretical results is provided, and additional information is presented.

METHODS

To obtain model spectra it is first necessary to calculate the evolution of the density operators associated with the compounds of interest, under the pulse sequence of interest. The evolution of the density operator is given by the Liouville–von Neumann equation:

$$\dot{\sigma} = -i\hbar[H, \sigma]. \qquad [1]$$

For this report only time-independent Hamiltonians, H, are considered. In this case, the solution to Eq. [1] is given formally by

$$\sigma(t) = e^{-Ht}\sigma(0)e^{Ht}. \qquad [2]$$

As discussed in the Introduction, spin evolution subject to the STEAM sequence is considered. Previous reports have demonstrated experimental and theoretical analyses (12), enabling convenient comparison with the results obtained. The STEAM sequence consists of three 90° pulses, with each pulse followed by gradient pulses as indicated in Fig. 1. Although the GAMMA package is capable of simulating realistic pulse shapes, for simplicity, and to facilitate comparison with the symbolic calculations, ideal (rectangular) RF pulses have been
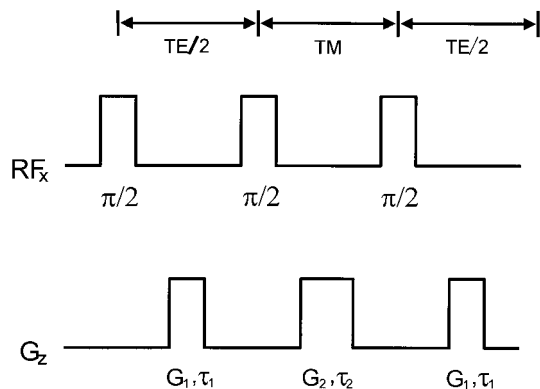

FIG. 1. Schematic of the STEAM pulse sequence. This shows RF pulses with the same phase, and gradient pulses in the z direction, as was used experimentally.

assumed. As in (12), it has been assumed that the gradient applied during the TM period was strong enough that only zero-order coherences (i.e., coherences that are insensitive to this gradient) could be refocused in the final TE/2 period, to generate observable signal.

To test the methods described below, the effect of the STEAM sequence on the lactate AX_3 system was studied. This spin system was selected because the product operator calculations under STEAM have been previously reported in the literature (12), yet the calculations are sufficiently complicated to constitute a meaningful test of both numeric simulations and symbolic product operator calculations.

Numerical Simulations Using GAMMA

The most efficient way of generating model spectra is via numerical simulation. For spin systems with more than five or six spins, numerical simulations are in fact the only practical means of obtaining theoretical spectra as analytical calculations are simply too difficult. In this report, simulation of the STEAM experiment is facilitated by introducing efficient methods for simulation of the effects of the gradients applied between the RF pulses into the GAMMA package.

To simulate STEAM, consideration of spatially dependent gradient-induced phases for the spin coherences is necessary. Although the GAMMA package does not specifically provide this functionality, it can be added simply by performing a large number of simulations for spin systems with different effective spectrometer frequencies during the gradient periods, and combining the results. However, this approach can be very time-consuming. Simulation of the effect of a gradient requires simulations at hundreds of points (in each spatial dimension for localization sequences). For example, a typical single GAMMA simulation of STEAM for a four-spin system takes on the order of tens of seconds (on a SPARC 20). Thus, the use of hundreds of individual simulations (for the gradient values) would require on the order of hours for simulation of a single

pulse sequence that included gradients, for a four-spin system. Given that one of the potentially important applications of these methods is to search for optimal values for multiple sequence parameters for observation of a variety of spin systems, significant reductions in simulation times are useful. In this report advantage is taken of insights gained from the product operator calculations regarding coherence transfer to generate a computationally efficient simulation scheme for simulating gradients, and therefore for simulating STEAM.

The effects of the gradients in the initial and final TE periods, shown in Fig. 1, are to change the phase of terms of coherence order p by an amount $-p\gamma(\mathbf{G} \cdot \mathbf{r})t$, where γ is the gyromagnetic ratio of the nucleus being considered, $\mathbf{G}$ is the gradient vector, $\mathbf{r}$ is the position vector of the spin system, and t is the duration of the gradient pulse. A straightforward way of simulating the gradients, i.e., the effects of the $\mathbf{G} \cdot \mathbf{r}$ term, would be to specify a set of effective spectrometer frequencies in GAMMA, corresponding to a set of spatial locations. Instead, the assumption that the gradient strengths and durations are sufficient to produce zero net transverse magnetization is used. As indicated above, each coherence order above zero can be viewed as a vector quantity with an associated phase. Thus, the effect of a gradient pulse is to produce a distribution of phases for each coherence order above zero, with the phase angle depending upon the spatial position of the spins. To simulate the effect of the gradients, we may consider just the projections of the individual coherences upon the x and y coordinate axes in the rotating frame. The initial magnetization is represented by coherence terms of order zero. As there are no coherence order zero terms following the first 90° pulse, the effect of the first gradient is to distribute the coherences such that there are equal projections about the x, y, $-x$, and $-y$ axes. Each coherence projection is reduced by the factor $2/\pi$ from the original coherence magnitude. The fate of each projection is then followed by separate GAMMA simulations. For each of the projections, the second 90° pulse can produce zero- and higher-order coherences, but the gradient during the TM period effectively destroys all but the zero-order coherences. Following the third 90° pulse, the final gradient adds additional phase equal to that produced by the initial gradient. This reduces the coherence projection by a factor of $\pi/4$, without producing any net projections in other directions. Note that the net reduction is the product of the individual reductions $(2/\pi)(\pi/4) = \frac{1}{2}$, i.e., the familiar net decrease in amplitude of $\frac{1}{2}$ for the STEAM sequence.

In summary, the effect of the gradients was simulated by using only four separate GAMMA simulations rather than hundreds or thousands. Each successive simulation consisted of an incremental rotation of $\pi/2$ about the z axis, following the first and third 90° pulses. The results of the four simulations were summed. The correct magnetization magnitude was maintained by: (1) reducing the non-zero-order coherences following the first gradient pulse by $2/\pi$, (2) zeroing all non-zero-order coherences following the second 90° pulse to sim-

ulate the effects of the the TM gradient, and (3) further reducing coherence projections by $\pi/4$ following the last 90° pulse. Zeroing of non-zero-order coherences during TM was possible because GAMMA provides functions that enable manipulation of individual coherence orders.

To perform simulations for a particular spin system, GAMMA requires chemical shifts and coupling values as input. For the simulations reported here, the following values, obtained by line-fitted analysis of lactate spectra using the Nuts program (Acorn NMR Inc., Fremont, CA), were used: $\sigma_1 = 4.0908$ ppm, $\sigma_{2,3,4} = 1.3125$ ppm, and $J = 6.933$ Hz. Given these values, simulations were performed for lactate, using the method described to simulate STEAM. To compare with the experimental data three sets of simulations were performed. The first set consisted of spectra for 1000 TE values between 7 and 300 ms at a fixed TM value of 70 ms. The second set consisted of spectra for 1000 TE values between 7 and 300 ms at a fixed TM value of 12 ms. To investigate the oscillations due to coupling at high resolution relative to the period, the third set consisted of spectra for 1000 TE values between 10 and 20 ms at a fixed TM value of 12 ms. For each data set the doublet signal was obtained by integrating each spectrum between 0.8 and 2.0 ppm. In addition, the effect of a T2 exponential decay were added to match simulation and experimental data.

Algebraic Analysis Using Mathematica

To verify the numerically simulated results, as well as confirm the form of the analytic calculation derived by Wilman and Allen for the lactate spectrum obtained using STEAM (12), product operator calculations were performed symbolically using Mathematica. These were based on the script developed by Shriver (7), with several modifications added. In particular the script was extended to handle calculations for the AX_3 system and the STEAM dephasing gradients. In addition, minor corrections such as sign corrections to the original script were added.

To simplify density operator calculations, the product operator formalism was introduced in (14). The basic principle underlying the product operator formalism is that the density operator can be expanded in basis operators, $\mathbf{B}_k$,

$$\sigma(t) = \sum_{k=1}^{K} b_k(t)\mathbf{B}_k \qquad [3]$$

and that the basis operators can be chosen in a way that is convenient for a particular problem. For the Mathematica script used in this report, the basis operators, $\mathbf{B}_k$, consist of combinations of spherical angular momentum operators that provide a convenient basis for tracking changes in coherence order. Density operator calculations can then be carried out using the operator algebra, and the calculated quantities are
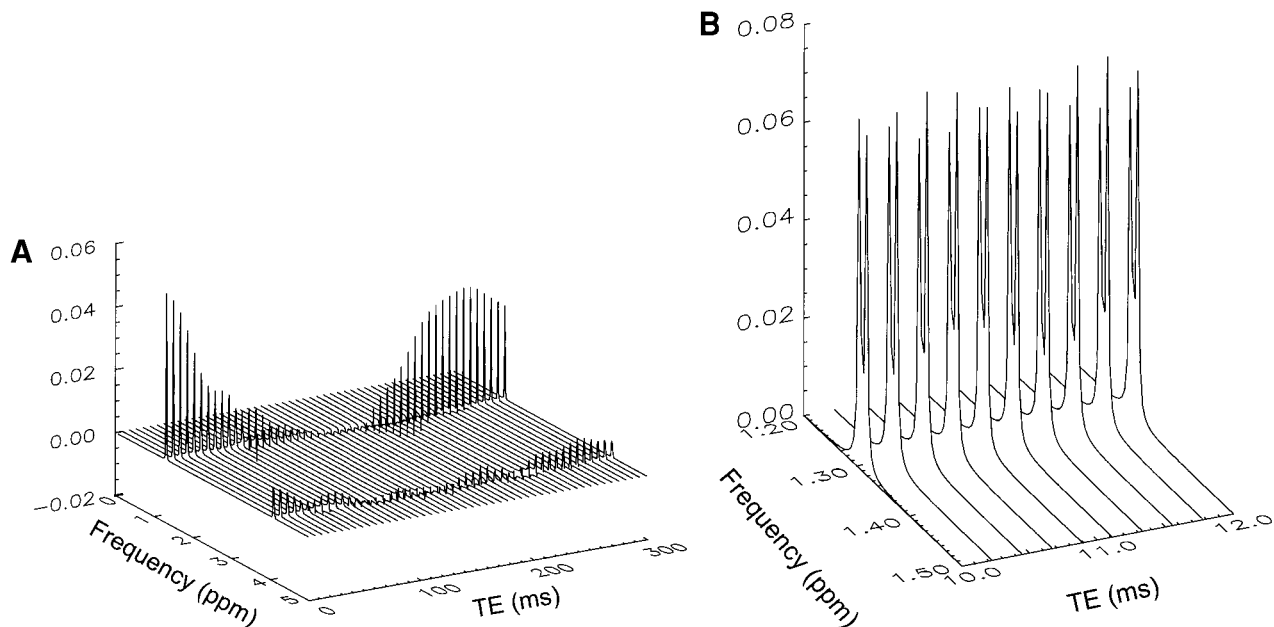
FIG. 2. (A) Stackplot of GAMMA simulations for the STEAM sequence of lactate as a function of TE, and a fixed TM value of 12 ms. The plot illustrates the variation in amplitude of the doublet and quartet resonance groups due to the combined effects of chemical shift and coupling evolution. (B) Stackplot of the evolution of the doublet resonance group for TE values between 10 and 12 ms, and a fixed TM value of 12 ms. The plot illustrates the phase variation of the doublet described in the main text and that occurs at a frequency $\delta\omega/2 \approx 1.7$ kHz.

related directly to experimental results. For a general introduction to product operator methods see (15).

The extension to handle the AX_3 system consisted of adding the appropriate rules for operator evolution under weak coupling for an AX_3 spin system (16). For example, using the rules given in (16) the following coupling evolution rule for the $I_+S_-^i$ product of spherical angular momentum operators can be written as

$$I_+S_-^i \xrightarrow{\quad JI_0(S_0^1 + S_0^2 + S_0^3) \quad}$$

$$I_+S_-^i(\cos(\pi Jt) - 2iS_0^j\sin(\pi Jt))$$
$$\times (\cos(\pi Jt) - 2iS_0^k\sin(\pi Jt)), \quad i \neq j \neq k \quad [4]$$

where the operator I acts on the A spins and the operator S acts on the X spins.

The extension to handle gradients consisted of adding various selection rules. One of the selection rules served to eliminate nonzero coherence order terms during the TM evolution. Another eliminated multiple product operator terms that had no possibility of yielding observable terms, given the remaining set of RF and gradient pulses. For example, one of the terms obtained in the expansion of the evolution rule in Eq. [4] is $-4I_+S_-^iS_0^jS_0^k\sin^2(\pi Jt)$. This term has zero coherence order and survives the TM gradient. Noticing, however, that no single coherence order (i.e., observable) terms result from the application of the remaining RF and gradient pulses, this term

can be eliminated, reducing the number of terms carried in the remaining calculations.

Many of the symbolic techniques described in this report generalize to arbitrary spin systems, e.g., inclusion of the effects of gradients and operators that eliminate unobservable terms. Nonetheless, generalization of the Mathematica script to other spin systems is more difficult than the straightforward generalization of the numerical simulations. This is because symbolic calculations generally require a significant amount of intervention to reduce and transform algebraic expressions at each step of a calculation. It is difficult to anticipate all the algebraic forms that will occur and need to be simplified and/or transformed at each step without following the calculation step by step. While the basic operations for the product operator calculations generalize, calculations for any particular spin system require that a number of specialized operations be developed in addition to the basic operations. This is not the case for GAMMA simulations; once a technique has been developed, it is applicable to any spin system.

Experimental Methods

Experimental data were obtained on a 14-T NMR spectrometer (Varian UNITY INOVA). The STEAM sequence used consisted of three 90° nonselective rectangular pulses of duration 6.15 μs, a TE/2 interval gradient of 1.01 ms duration and 10.123 mG/cm (along the Z axis), a TM interval gradient of 8 ms and 11 mG/cm (along the Z axis), 16K data points, a spectral width of 4 kHz, and a sequence repetition delay of
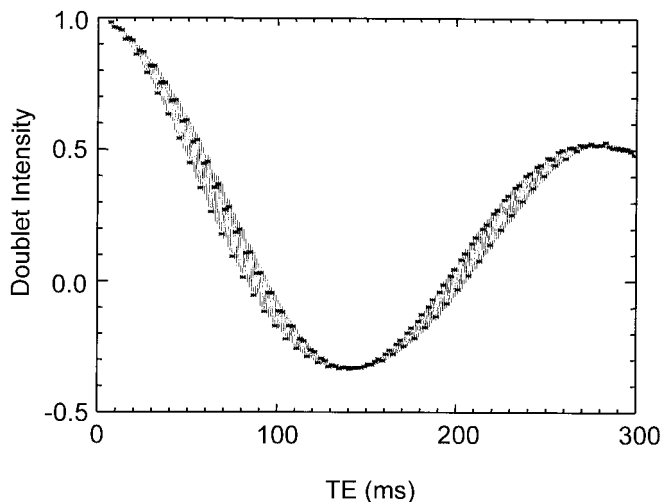
FIG. 3. Plot of the signal integral of the lactate doublet as a function of TE, at TM = 12 ms. The acquired data values (asterisks) are compared with the GAMMA simulation (solid line).

15 s. The sample used was a 5-mm NMR tube containing 100 mM lactate solution prepared in D_2O at pH 7.0 (6.6 meter reading). Spectra were acquired with TM values of 12 and 70 ms, at a temperature of 37°C, without sample spinning. For each TM value, spectra were acquired for 148 TE values starting at 7 ms and incremented in steps of 2 ms. An additional data set was acquired for TM = 12 ms, using 100 TE values starting with 10 ms and incremented in steps of 100 μs. Each data file was zero filled and Fourier transformed. The doublet signal integral was obtained by integrating each spectrum between 0.8 and 2.0 ppm, and normalizing the integral values to the integral value obtained at the smallest TE value.

RESULTS

The results of the Mathematica calculation agree with that derived in (12), aside from a typographical error (the minus sign in front of the last exponential term in Eq. [4] of (12)). The intensity of the doublet as a function of TE is given as

$$
S(\text{TE}) = \frac{1}{2} \left\{ \cos^2\left(\frac{J\pi\text{TE}}{2}\right) - \frac{1}{2} \sin^2\left(\frac{J\pi\text{TE}}{2}\right) \right.
$$

$$
\times \left(1 - \frac{1}{2} \cos^2\left(\frac{J\pi\text{TE}}{2}\right) \exp\left(\frac{i\delta\omega\text{TE}}{2}\right) \right)
$$

$$
\left. \times \cos^2(J\pi\text{TM})\cos(\delta\omega\text{TM}) \right\}, \qquad [5]
$$

where $\delta\omega$ is the frequency difference between the quartet and the doublet. We maintain both real and imaginary parts of the intensity in Eq. [5] because, as discussed below, the phase of the doublet signal has an observable effect.

The variation in the amplitudes of the lactate multiplets as a

function of TE, for the STEAM sequence with TM = 12 ms, are shown in Fig. 2. The overall variation is composed of a superposition of terms with different frequencies in agreement with Eq. [5]. Two significant terms vary as a function of TE. The first, with frequency $J\pi/2$, is a function of the coupling and governs the overall shape of the integrated signal amplitude variation as a function of TE. The second, with frequency $\delta\omega/2$, is a function of the chemical shift difference and the spectrometer frequency and governs the observed high-frequency oscillations.

The results of the GAMMA simulation produce doublet intensity variations that are essentially identical to Eq. [5]. Therefore, in the figures only the results of the GAMMA simulations are shown and compared with the experimental data. The Mathematica code is available from the authors.

In Fig. 3 is shown the integrated doublet intensity as a function of TE for STEAM with TM = 12 ms for the GAMMA simulation (dark line) and the data (asterisks). The agreement in terms of the overall shape appears excellent, though on this scale the high-frequency oscillations are hard to resolve. In Fig. 4 is shown a detailed view of the region between TE = 10 ms and TE = 20 ms. The data in this case were taken at an interval of 100 μs. Even on this scale there is excellent agreement between the simulation and the experimental data. In this case, the high-frequency oscillation at $\delta\omega/2 \approx 0.8$ kHz is well resolved. As discussed in (12) and confirmed from our Mathematica analysis, at a value of TM = $1/2J$ the high-frequency oscillations vanish. This can be seen in Fig. 5, where the integrated doublet intensity is plotted as a function of TE, with TM = 70 ms $\approx 1/2J$, for the GAMMA simulation (dark line) and the data (asterisks). This effect is relatively insensitive to small changes in TM about TM = $1/2J$, since, as can be seen from Eq. [5], there is a relatively broad minimum of the function $\cos^2(J\pi\text{TM})$. This accounts for the relatively good agreement between theory and experiment in (12) despite the
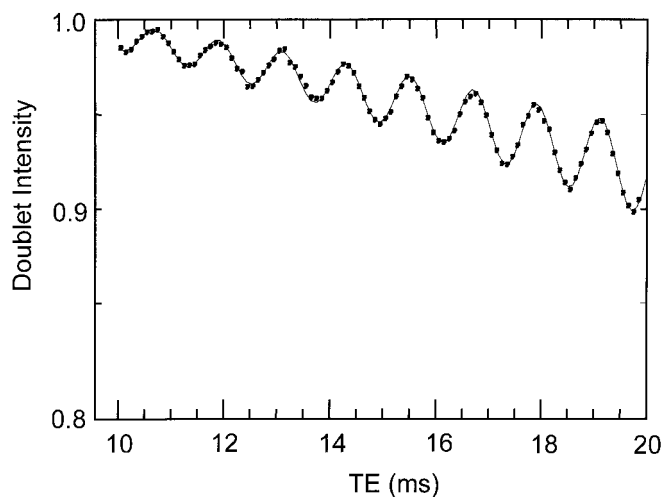

FIG. 4. Enlarged view of the data integral shown in Fig. 3, for the TE range of 10 to 20 ms.
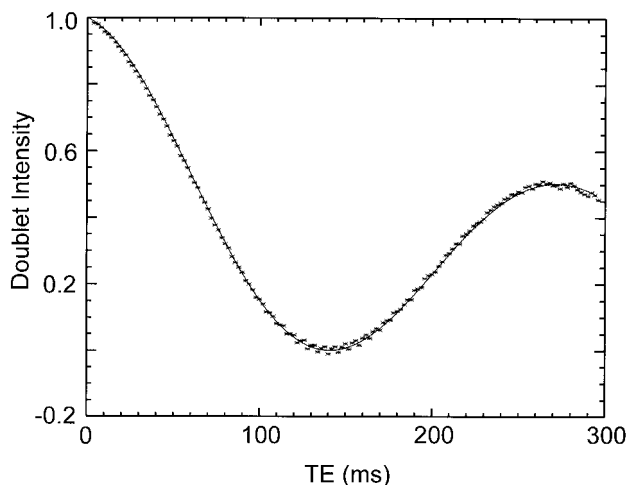
FIG. 5. Plot of the signal integral as a function of TE. Data (asterisks) and GAMMA simulation results (solid line) are plotted for TM = 70 ms.

use of a coupling value of TM = 70 ms rather than the more accurate value of $1/2J \approx 72$ ms as determined by our measurements.

Finally, as can be seen in Eq. [5], there is also a phase variation in the doublet, depending on TE, with frequency $\delta\omega/2$. This variation is also visible in Fig. 2. While not large, this phase variation would be significant in generating correct basis functions for spectral fitting.

DISCUSSION

In this report, two computational methods, numerical simulation and symbolic computation, have been presented to simulate a NMR response subject to the effects of magnetic field gradients for dephasing and rephasing. The use of these methods avoids the tedious algebra associated with the direct calculation of complex spin systems with the product operator formalism and facilitates the generation of reliable results. This work has extended two existing software packages. Both of the extended packages were tested by modeling the response of an AX_3 spin system to excitation by the STEAM pulse sequence with one-dimensional spatial localization, and by comparison with experimental results. In both cases, excellent agreement between simulation and experimental results was obtained. In addition, the results have also been compared with a previously published theoretical analysis, again with complete agreement, together with inclusion of the imaginary component in the result. Although the application considered in this report has been simulation of spectra acquired using a specific spatial localization method, these results can be generally applied to other NMR pulse sequences. This includes methods that use magnetic field gradients for coherence selection and three-dimensional STEAM localization sequences.

The first method presented used an efficient extension of the GAMMA library to provide direct numerical simulation of spin responses to gradient dephasing and rephasing. The use of GAMMA, in general, is highly efficient in at least two ways. First, efficient use of GAMMA's well-designed object-oriented class libraries allows for rapid development of compact programs for testing the responses of a variety of compounds to a variety of pulse sequences. Second, the code generated using GAMMA is generally very efficient in terms of processing requirements. The extensions to GAMMA described in this report, which allow for efficient simulation of gradients, provide a significant increase in the set of pulse sequences that can be effectively investigated by numerical simulation.

The second method used an expanded Mathematica script to generate an analytical result using the product operator formalism. Although more computationally intensive, this latter method can provide greater insight into the mechanisms giving rise to the results, and for some applications this may offer an advantage. For example, to determine an optimal set of experimental parameters it may be sufficient to directly examine the analytical result, whereas numerical simulation would require repeated calculations to determine the optimum values. In its current form, however, additional programming is necessary before the symbolic algebra approach is generally applicable to all spin systems. Various difficulties, e.g., including the effects of gradients and generating the algebraic operations for elimination of nonobservable terms, currently limit the size of spin systems that can be accommodated with available computer resources. In comparing the numerical and symbolic methods it is important to note that the symbolic methods are significantly more difficult to generalize to arbitrary spin systems as well as being more computationally resource intensive. For GAMMA simulations, once the chemical shifts and couplings for a spin system are specified, GAMMA internally constructs the appropriate Hamiltonian and evolves the density matrix. No changes in the simulation code are required to handle different spin systems. If only the generation of simulated spectra is required, and no examination of intermediate steps in the calculation is required, numerical simulation is clearly the method of choice.

An important application of this work has been the generation of *a priori* information for tissue metabolite spectra observed using spatial localization methods. Determining the amplitudes of low-concentration metabolites from typical noisy, overlapped spectra is generally very difficult. The ability to perform the density matrix calculations for the response of the tissue metabolites to the experimental pulse sequence provides significant *a priori* information that can be used for fitting the metabolite peaks. For this application, numerical simulations are performed to obtain the responses of the set of metabolites of interest to the experimental pulse sequence. The outcome of the simulations is a set of basis functions to be used in a parametric spectral analysis procedure. By using the numerical simulation methods presented in this report, spectral results can be obtained not only for the STEAM acquisition sequence but also for a number of pulse sequences that provide multiple-quantum observation. Using numerical simulation,

the required *a priori* information can be rapidly generated with minimal user interaction. For either numerical simulation or symbolic calculation, an additional potential application is optimization of pulse sequence parameters to emphasize the signal of specific spin systems, in the presence of overlapping resonances from other compounds (*10*). The authors will be pleased to provide the GAMMA simulation code and the Mathematica script upon request.

REFERENCES

1. R. R. Ernst, J. Bodenhausen, and A. Wokaun, "Principles of Nuclear Magnetic Resonance in One and Two Dimensions," Clarendon Press, Oxford (1987).
2. A. Wokaun and R. R. Ernst, *Chem. Phys. Lett.* **52**, 407–412 (1977).
3. K. Young, V. Govindaraju, B. J. Soher, and A. A. Maudsley, *Magn. Reson. Med.* **40**, 812–815 (1998).
4. J. Shane, L. Lorenz, and A. Schweiger, *J. Magn. Reson.* **134**, 72–75 (1998).
5. S. A. Smith, T. O. Levante, B. H. Meier, and R. R. Ernst, *J. Magn. Reson. A* **106**, 75–105 (1994).
6. R. B. Thompson and P. S. Allen, *Magn. Reson. Med.* **39**, 762–782 (1998).
7. J. Shriver, *Concepts Magn. Reson.* **4**, 1–33 (1992).
8. A. M. N. Jerschow, *J. Magn. Reson.* **134**, 17–29 (1998).
9. K. Young, B. J. Soher, and A. A. Maudsley, *Magn. Reson. Med.* **40**, 816–821 (1998).
10. V. Govindaraju, K. Young, G. B. Matson, and A. Maudsley, submitted for publication (1998).
11. J. Frahm, K. D. Merboldt, and W. Hänicke, *J. Magn. Reson.* **72**, 502–508 (1987).
12. A. H. Wilman and P. S. Allen, *J. Magn. Reson.* **101**, 102–105 (1993).
13. P. Guntert, N. Schaefer, G. Otting, and K. Wuthrich, *J. Magn. Reson.* **101**, 103–105 (1993).
14. O. W. Sørensen, G. W. Eich, M. H. Levitt, G. Bodenhausen, and R. R. Ernst, *Prog. NMR Spectrosc.* **16**, 163–192 (1983).
15. J. Cavanagh, W. J. Fairbrother, A. G. Palmer, and N. J. Skelton, "Protein NMR Spectroscopy: Principles and Practice," Academic Press, San Diego (1996).
16. L. E. Kay and R. E. D. McClung, *J. Magn. Reson.* **77**, 258–273 (1988).